Louisiana State University

LSU Digital Commons

4-21-2015

The relationship between X-ray luminosity and duty cycle for dwarf novae and their specific frequency in the inner Galaxy

C. T. Britt
Texas Tech University

T. Maccarone
Texas Tech University

M. L. Pretorius
University of Oxford

R. I. Hynes
Louisiana State University

P. G. Jonker
SRON Netherlands Institute for Space Research

See next page for additional authors

Follow this and additional works at: https://digitalcommons.lsu.edu/physics_astronomy_pubs

Recommended Citation

Authors

C. T. Britt, T. Maccarone, M. L. Pretorius, R. I. Hynes, P. G. Jonker, M. A.P. Torres, C. Knigge, C. O. Johnson, C. B. Heinke, D. Steeghs, S. Greiss, and G. Nelemans

The relationship between X-ray luminosity and duty cycle for dwarf novae and their specific frequency in the inner Galaxy

C. T. Britt,[1]⋆ T. Maccarone,[1] M. L. Pretorius,[2] R. I. Hynes,[3] P. G. Jonker,[4,5,6]
M. A. P. Torres,[4,5] C. Knigge,[7] C. O. Johnson,[3] C. B. Heinke,[8,9] D. Steeghs,[10]
S. Greiss[10] and G. Nelemans[5]

[1]*Department of Physics, Texas Tech University, Box 41051, Science Building, Lubbock, TX 79409-1051, USA*
[2]*Department of Physics, Oxford University, Denys Wilkinson Building, Keble Road, Oxford OX1 3RH, UK*
[3]*Department of Physics and Astronomy, Louisiana State University, Baton Rouge, LA 70803-4001, USA*
[4]*SRON, Netherlands Institute for Space Research, Sorbonnelaan 2, NL-3584 CA Utrecht, the Netherlands*
[5]*Department of Astrophysics, IMAPP, Radboud University Nijmegen, Heyendaalseweg 135, NL-6525 AJ Nijmegen, the Netherlands*
[6]*Harvard–Smithsonian Center for Astrophysics, 60 Garden Street, Cambridge, MA 02138, USA*
[7]*School of Physics and Astronomy, University of Southampton, Hampshire SO17 1BJ, UK*
[8]*Physics Department, University of Alberta, CCIS 4-183, Edmonton, AB T6G 2E1, Canada*
[9]*Max-Planck-Institute für Radioastronomie, Auf dem Hügel 69, D-53121 Bonn, Germany*
[10]*Astronomy and Astrophysics, Department of Physics, University of Warwick, Coventry CV4 7AL, UK*

ABSTRACT

We measure the duty cycles for an existing sample of well-observed, nearby dwarf novae (DNe) using data from American Association of Variable Star Observers, and present a quantitative empirical relation between the duty cycle of DNe outbursts and the X-ray luminosity of the system in quiescence. We have found that $\log \mathrm{DC} = 0.63(\pm 0.21) \times (\log L_X(\mathrm{erg\,s^{-1}}) - 31.3) - 0.95(\pm 0.1)$, where DC stands for duty cycle. We note that there is intrinsic scatter in this relation greater than what is expected from purely statistical errors. Using the DN X-ray luminosity functions from Pretorius & Knigge and Byckling et al., we compare this relation to the number of DNe in the Galactic Bulge Survey which were identified through optical outbursts during an 8-d-long monitoring campaign. We find a specific frequency of X-ray-bright ($L_X \gtrsim 10^{31}\,\mathrm{erg\,s^{-1}}$) cataclysmic variables (CVs) undergoing DNe outbursts in the direction of the Galactic bulge of $6.6 \pm 4.7 \times 10^{-5}\,M_\odot^{-1}$. Such a specific frequency would give a solar neighbourhood space density of long-period CVs of $\rho = 5.6 \pm 3.9 \times 10^{-6}\,\mathrm{pc^{-3}}$. We advocate the use of specific frequency in future work, given that projects like Large Synoptic Survey Telescope will detect DNe well outside the distance range over which $\rho \approx \mathrm{const}$.

Key words: accretion, accretion discs – stars: dwarf novae – novae, cataclysmic variables.

1 INTRODUCTION

Cataclysmic variables (CVs) are binary star systems in which a white dwarf (WD) primary accretes material from a low-mass secondary star through Roche lobe overflow. In the absence of strong magnetic fields of the WD, the infalling material forms an accretion disc, through which angular momentum can be transferred between particles allowing accretion on to the surface of the WD.

The material in the disc heats as it builds up, eventually reaching the ionization temperature of hydrogen. At this point, the gas in the disc becomes much more viscous (Smak 1999; Lasota 2001). The heat energy from the increase in viscosity causes a heating wave to propagate through the disc, ionizing the remainder of it. Mass then passes through the high-viscosity disc at a much higher rate, dumping material on to the WD. A sudden brightening of several magnitudes and subsequent decline to the original brightness is observed over the course of days to weeks (Smak 1971; Warner & Nather 1971). These dwarf novae (DNe) occur with a frequency tied to the recent mass accretion rate $\dot{M}_1$ and mass transfer rate $\dot{M}_2$ of the system, as the disc must refill in between outbursts. High-mass transfer rate CVs (nova-like objects) do not undergo DNe as the discs are constantly above the ionization temperature of hydrogen. Low mass transfer rate objects such as WZ Sge may go decades between recurrences of DN outbursts.

The mass accretion rate in CVs is also known to be tied to X-ray luminosity up to a critical rate at which point the boundary layer (BL) on the surface of the WD becomes opaque to X-rays (Patterson & Raymond 1985; Wheatley, Mauche & Mattei 2000; Baskill, Wheatley & Osborne 2001). Indeed, the X-ray emission

during a DN outburst can rise at the start of the outburst as for SS Cyg until the BL becomes opaque at which point the X-rays are quenched. Some DNe never reach this critical accretion rate and the X-ray emission remains unquenched through the duration of the outburst (e.g. U Gem; Swank et al. 1978).

The empirical population of CVs can constrain evolution models; a crucial measurement to make with this end in mind is the space density of CVs, ρ. Models of binary evolution predict space densities ranging over an order of magnitude or more, from 10^{-5} to 10^{-4} pc^{-3} (de Kool 1992; Kolb 1993; Politano 1996). Observational campaigns, largely using X-ray-selected samples, have made estimates of the CV space density converging on 0.5–1×10^{-5} pc^{-3} (Patterson 1998; Schreiber & Gänsicke 2003; Aungwerojwit et al. 2006; Pretorius et al. 2007; Rogel, Cohn & Lugger 2008; Pretorius & Knigge 2012). The space density found in Pretorius & Knigge (2012) for long-period CVs was $2.1^{+3.5}_{-1.3} \times 10^{-6}$ pc^{-3} which assumed that all systems with unknown periods had periods below the period gap. Studies of the space density of CVs have focused on the solar neighbourhood, for the simple and expedient reason that a complete census of faint CVs will be impossible to acquire at large distances. The outlier among estimates of space density from observational campaigns, finding a much smaller space density for the DN population ($<5 \times 10^{-7}$ pc^{-3}), used the Optical Gravitational Lensing Experiment (OGLE) survey towards the Galactic bulge to find DN outbursts (Cieslinski et al. 2003). This estimate was based on identifying distant DN outbursts as part of a larger wide-field survey as is this work, where Cieslinski et al. (2003) uses the OGLE-II survey and this work is based on the *Chandra* Galactic Bulge Survey (GBS).

The GBS is an X-ray survey between $-3° < l < 3°$ and $1° < |b| < 2°$ with shallow coverage of 2 ks (Jonker et al. 2011, 2014). The primary goal of the GBS is to conduct a census of low-mass X-ray binaries in quiescence (qLMXB), in order to constrain models of binary evolution and to identify new systems for which mass determinations are possible, including eclipsing systems. Towards the goal of classifying each X-ray source in the GBS, multiwavelength photometric and spectroscopic follow-up campaigns have been undertaken. Some of these focus on classifying new interesting sources with detailed follow-up, such as new CVs (Britt et al. 2013; Ratti et al. 2013), a possible new black hole binary (Britt et al. 2013), a slowly pulsating B star with a WD or coronally active G-type companion (Johnson et al. 2014), and a likely carbon star symbiotic binary (Hynes et al. 2014). In terms of more comprehensive follow-up, Britt et al. (2014) focus on variable optical counterparts to GBS sources including the identification of DNe in outburst; Greiss et al. (2014) identify the infrared counterparts; Hynes et al. (2012) cross match GBS sources with bright star catalogues such as *Tycho* and ASAS; Maccarone et al. (2012) cross match GBS sources with existing catalogues of radio sources; Torres et al. (2014) and Wu et al. (2015) provide optical spectroscopy of stars with an Hα excess near GBS sources. The initial X-ray survey, which covered 3/4 of the planned survey area, discovered 1216 unique X-ray sources with three or more detected photons in a 2 ks observation. The X-ray observations were kept intentionally shallow in order to keep the number of active stars and CVs in the survey low while still reaching the bulge for neutron star and long-period black hole qLMXBs. As a result, the non-magnetic CVs in the GBS are generally closer than bulge distance. For example, the X-ray bright system Z Cam would be detected up to ∼4500 pc away.

Our use of an optical variability survey as part of the GBS to constrain the space density of CVs in the direction of the Galactic bulge mirrors in some ways that undertaken with the OGLE-II catalogue in Cieslinski et al. (2003). Our survey differs in several key respects. First, our analysis takes into account the likelihood of detecting DNe with recurrence times much longer than the baseline of observations. Not allowing for DNe with recurrence periods longer than the OGLE time baseline is the likely reason why Cieslinski et al. (2003) obtained a final DN space density much lower than that obtained by other methods, or that we find in this paper. Secondly, the limiting magnitude in our survey is slightly deeper than that of OGLE-II, $r' = 23$ versus $I = 22$, though this is equalized by reddening. Thirdly, our baseline of observations is dramatically shorter than in OGLE-II, with an 8 d baseline compared to OGLE-II's four years of observations, though both are shorter than the recurrence time of many CVs undergoing DN outbursts and are therefore far from complete samples. Fourthly, our optically surveyed area is currently somewhat smaller, 9 deg^2 (Britt et al. 2014) instead of OGLE-II's 12. Lastly, our optical detections of DNe, at the present time, are premised on an X-ray detection of the same CV. Recent progress in determining the X-ray luminosity function of CVs combined with a more complete sample of well observed, nearby DNe allows our sample to be leveraged in ways that were not available at the time of OGLE-II as well. Cieslinski et al. (2003) place an upper limit on the space density of CVs towards the Bulge of 5×10^{-7} pc^{-3}. In this work, we reconcile recent estimates of the X-ray-selected CV space density with an optical-outburst-selected DN space density.

2 DUTY CYCLE VERSUS X-RAY LUMINOSITY

2.1 Sample selection and measurements for duty cycle versus luminosity relation

As a basis for determining the relationship between X-ray luminosities of CVs and other key properties, we use the survey of DN within ∼200 pc in Byckling et al. (2010). This sample, although small (13 CVs), includes only objects with accurate distance measurements from trigonometric parallax. Byckling et al. (2010) demonstrate that this sample is likely suffering from selection effects against low luminosities ($L_X < 3 \times 10^{30}$ erg s^{-1} in the [2–10] keV band) and duty cycles. We therefore limit our fit to the CVs with an X-ray luminosity above this cutoff. This sample is not distance complete, as it is limited to sources with parallax measurements which were mostly done by the same group with Northern hemisphere telescopes (Thorstensen 2003; Harrison et al. 2004; Thorstensen, Lépine & Shara 2008). As an exercise, we have fit the entire sample as well and find the resulting relation to be consistent with the more narrowly defined sample.

Since the publication of Byckling et al. (2010), the distance to SS Cyg has been revised downwards by the improved parallax measure in Miller-Jones et al. (2013), from 159 ± 12 to 114 ± 2 pc. This results in a drop in the X-ray luminosity by a factor of about 2 compared to the value listed in Byckling et al. (2010).

Each of these CVs is well observed, with decades of publicly available data in multiple surveys. Where available, we use published values of duty cycles extant in the literature. For other objects, we use American Association of Variable Star Observers (AAVSO) data in all available filters to measure the duty cycle of each CV in this sample, with results shown in Table 1. The AAVSO data are generally accurate to within 0.2 mag for individual observations (Henden 2014) and is much better for many simultaneous observations. We define the duty cycle as the number of days during which the source is in outburst divided by the total baseline of observations. We define outburst as an event reaching at least

Table 1. The measured duty cycles and extant X-ray luminosities for nearby DNe. To fit a relation between duty cycle and X-ray luminosity, we use only those DN with $L_X > 3 \times 10^{30}$ erg s^{-1}.

System	log L_X [2–10 keV] (erg s^{-1})	log duty cycle	P_{orb} (h)	References[a]
BZ Uma	31.17 ± 0.23	-1.39 ± 0.08	1.63	1
HT Cas	30.79 ± 0.21	-1.85 ± 0.12	1.77	1
SS Aur	30.982 ± 0.095	-0.61 ± 0.07	4.39	1
SW Uma	30.69 ± 0.15	-1.10 ± 0.14	1.36	1
U Gem	30.919 ± 0.053	-0.90 ± 0.02	4.25	1
T Leo	30.81 ± 0.13	-1.17 ± 0.16	1.42	1
V893 Sco	31.70 ± 0.31	-0.74 ± 0.12	1.82	1
SS Cyg	31.888 ± 0.066[b]	-0.53 ± 0.07	6.603	2,3
Z Cam	31.79 ± 0.33	-0.38 ± 0.05	6.98	4
GW Lib	28.7 ± 0.44	-2.34 ± 0.19	1.28	1,5
WZ Sge	29.85 ± 0.12	-1.85 ± 0.09	1.36	1
VY Aqr	30.11 ± 0.21	-2.17 ± 0.13	1.51	1
ASAS J0025	30.20 ± 0.42	$< -1.92 \pm 0.15$	1.37	1,6

Notes. [a]References: (1) Henden (2014) (2) Hamilton et al. (2007) (3) Miller-Jones et al. (2013) (4) Oppenheimer, Kenyon & Mattei (1998) (5) Maza & Gonzalez (1983) (6) Pojmanski (1997). [b]X-ray luminosities come from Byckling et al. (2010) in all cases but SS Cyg where we use a revised distance based on radio parallax.

2 mag greater than the quiescent magnitude beginning and ending when the object returns to 0.2 mag above the quiescent level prior to outburst. We do not include the standstills in Z Cam's high state as being in outburst; we consider only those times when Z Cam is in the low state and undergoing DN outbursts. We only include times at which the sources are visible and being observed consistently enough to be sure that no outbursts have been missed. Light curves of the data ranges used to measure duty cycle are presented in Fig. 1.

2.2 Fitting methods

Fitting a relation between the X-ray luminosities in the sample from Byckling et al. (2010) and the corresponding duty cycles is complicated by the presence of intrinsic scatter around the relation that is not represented by the statistical errors. Methods for dealing with these difficulties along with their strengths and shortcomings are discussed in Tremaine et al. (2002) and Kelly (2007). To account for the intrinsic scatter of the data, we add a systematic uncertainty to all duty cycle measurements that is calculated such that $\chi^2/\nu = 1$ for the initial fit by using the MPFITEXY routine (Williams, Bureau & Cappellari 2010) in the MPFIT package (Markwardt 2009). Without using this intrinsic scatter, $\chi^2/\nu = 15$ on the final best fit, which is a decidedly poor fit. Because the errors in the measurement of X-ray luminosity are somewhat asymmetric, we symmetrize them in log space. The changes in the errors this causes are of the order of 10 per cent. We use a bootstrapping method to estimate the errors in the fit of the full data set, as the distribution of the bootstrapped fit results matches the error distribution of the best fit (Press et al. 2007). For the bootstrapped fits without including an intrinsic scatter term, $\chi^2/\nu = 11.8 \pm 8.4$, still well above the expected range of $\chi^2/\nu = 1 \pm \sqrt{2/\nu}$. In the bootstrapping analysis, the intrinsic scatter in the log of the duty cycle is on average $\sigma_{int} = 0.31 \pm 0.12$, which gives $\chi^2/\nu = 1.20$, which is within $\chi^2/\nu = 1 \pm \sqrt{2/\nu}$ for $\nu = 7$.

In order to estimate the errors in the relation, we fit the bootstrapped distribution of fits with a Gaussian and use the width of the Gaussian to estimate the error. The slope and intercept have been fit together in each iteration, with the intercept set to near the middle of the data to remove correlation between the intercept and the slope during the fitting.

The resulting best fit is

$$\log DC = 0.63 \pm 0.21 \times (\log L_X(\text{erg s}^{-1}) - 31.3) - 0.95(\pm 0.1),$$

shown in Fig. 2. Fitting all of the DN in the Byckling et al. (2010) sample gives a relation that is consistent with the one above, but which may be subject to selection effects against low duty cycle DN with $L_X < 3 \times 10^{30}$ erg s^{-1}, and is given by

$$\log DC = 0.65 \pm 0.08 \times (\log L_X(\text{erg s}^{-1}) - 30.5) - 1.50 \pm 0.14.$$

This relation is unaffected by the inclusion or removal of ASAS J002511+1217.2 (ASAS J0025 henceforth), which has only one observed outburst, in the sample. The fits are shown in Fig. 3.

3 THE GBS SAMPLE OF DNE

In the search for variability in candidate optical counterparts for the northern 3/4 of the GBS survey area, described in detail in Britt et al. (2014), eight X-ray sources were observed to undergo a DN outburst. Of these eight, only the brightest (CX18) has so far been the target of both follow-up spectroscopic observations and optical monitoring, where it was observed to undergo a subsequent DN outburst and to have an optical spectrum confirming that it is a non-magnetic CV (Britt et al. 2013). Two others, CX39 and CX87, have been targeted for spectroscopic follow-up which confirms their CV nature (Torres et al. 2014). The remaining five DNe (CX: 81, 298, 426, 476, 860) have X-ray, infrared and optical colours and flux ratios consistent, where available, with CVs undergoing DN outbursts in addition to the presence of a rise or decline of >1 mag over a few days. Half of the observed DN occur in the brightest 100 X-ray sources out of the 1216 source survey population. The variability survey in Britt et al. (2014) only examines stars coincident with X-ray positions in the GBS catalogue; the data exist to study all objects in the field, but the full analysis is computationally intensive and beyond the scope of this paper. The X-ray detections for the GBS cover the energy range [0.5–10] keV, and include detections which have at least three photons.

The optical observations were made with the Mosaic-II instrument on the Blanco 4-m telescope at CTIO in 2012 July. A description of the data reduction and photometry methods is given in Britt
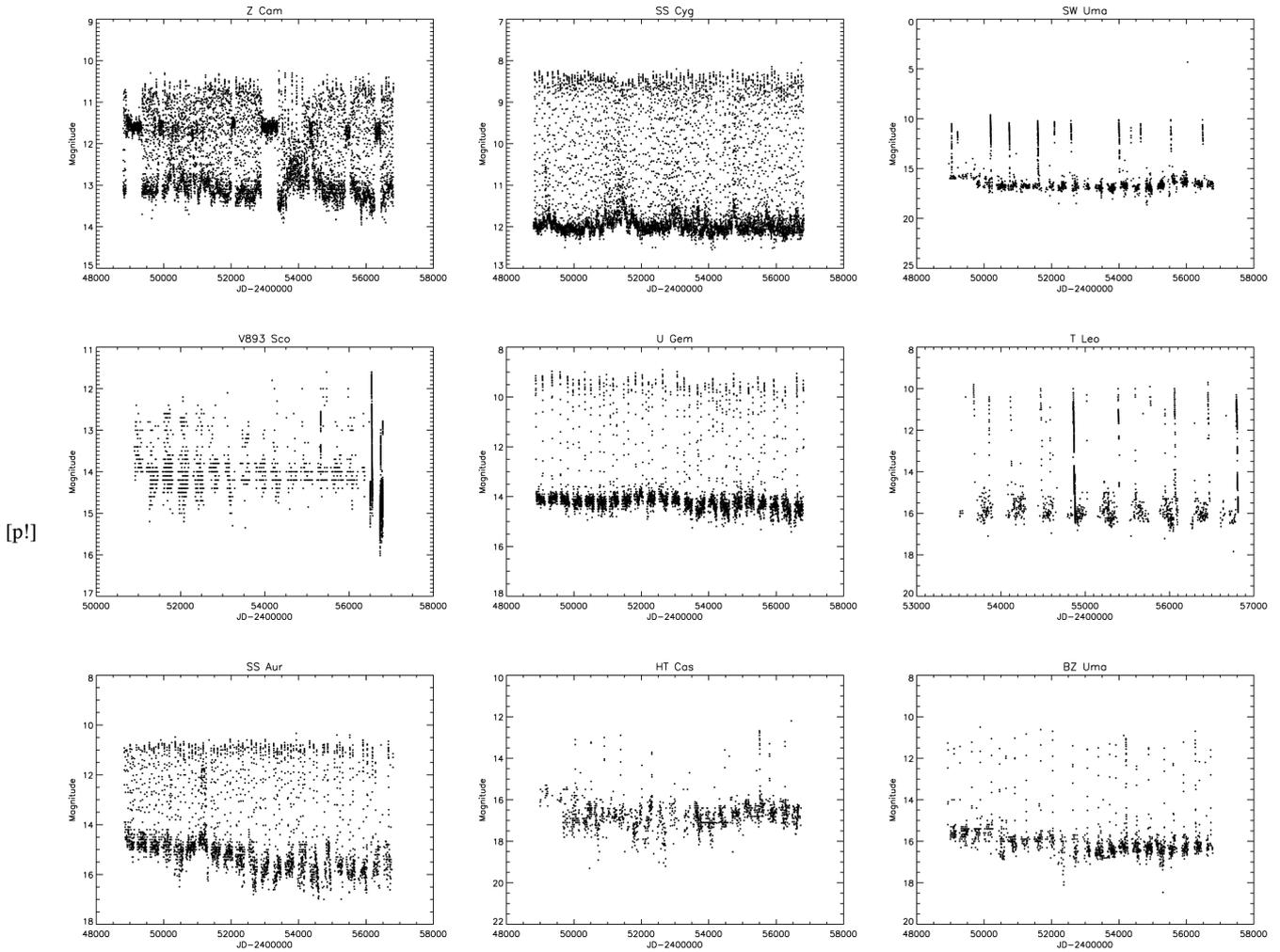
Figure 1. AAVSO light curves for DNe with parallax measurements within 200 pc. Here, we include only those sources with $L_X > 3 \times 10^{30}$ erg s^{-1} to avoid biases due to data incompletenesses at low L_X. Light curves for SS Cyg, U Gem and Z Cam have been binned to 1 d averages for clarity.
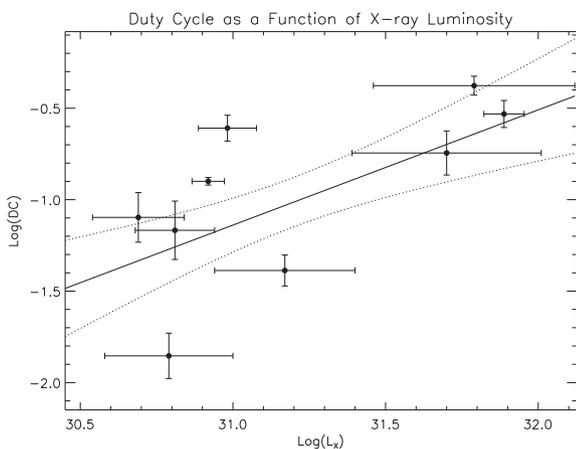
Figure 2. The best fit for duty cycle as a function of X-ray luminosity is plotted as a solid line. Dotted lines are the 1σ errors on this relation.

Figure 3. The best fit (solid line) and 1σ errors (dotted lines) between the duty cycles and X-ray luminosities of the entire sample in Byckling et al. (2010). The fit to the entire sample agrees well with the fit to only the X-ray bright sample, but it is likely that there is a strong sampling bias against low duty cycle DN below $L_X = 3 \times 10^{30}$ erg s^{-1}.

et al. (2014). The observations reach an optical depth of $r' = 23$ and span an 8 d baseline, which is long enough to notice either the sharp rise or slower decay of a DN outburst.

In addition to the eight objects classified as DN outbursts in Britt et al. (2014), there is one additional object, CX982, which could
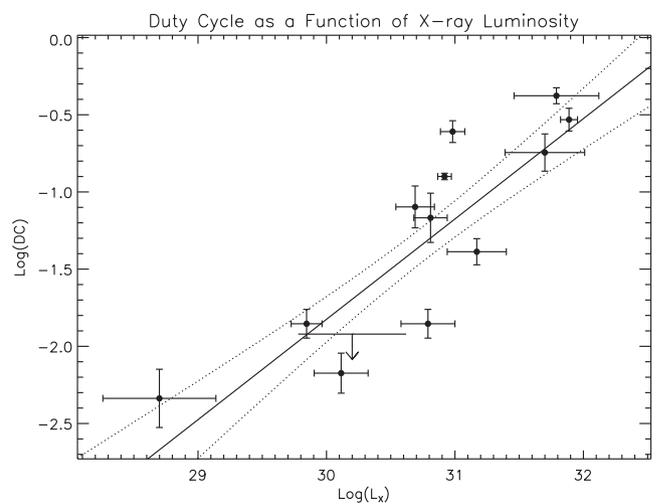
be a DN outburst with eclipses of the disc by the donor star during the outburst. It could also be some extreme coronal flaring, so we exclude it from our study here. If follow-up observations reveal that it is indeed a DN, the space density estimated will be too low by ∼12.5 per cent. To account for the chance that this object should be included in the sample, and for the smaller but non-zero chance that one or more of our DNe in the sample are, in fact, not DNe, we include an additional systematic error of 12 per cent in our final estimation of space density.

4 ESTIMATING SPACE DENSITY WITH MONTE CARLO SIMULATIONS

We can constrain the space density of CVs undergoing DN outbursts in the direction of the Galactic bulge by modelling a CV population which follows the X-ray luminosity function of Pretorius & Knigge (2012) and the duty cycle relation outlined above with various space densities, and comparing the resulting population with that seen by the GBS. We make several assumptions in this process.

(i) CVs trace stellar density in the disc, described by an exponential decay in both radius from the centre and height above the plane of the disc. We have considered three possible scalelengths of the disc in our simulations, 2.2, 3.0, 3.8 kpc to account for the continuing uncertainty in the details of Galactic structure (Jurić et al. 2008; Reylé et al. 2009). Changes to the scalelength did not impact our results in a significant way. In addition, we have considered a range of scaleheights of the disc. Because the scaleheight assumed had some impact on the results, we make the uncertainty of the true CV distribution a part of the simulation by adding a random component with a variance of 15 pc to a disc scaleheight centred on 120 pc (Pretorius & Knigge 2012). We assumed a distance to the Galactic Centre of 7620 pc (Eisenhauer et al. 2005).

(ii) The peak absolute magnitude of a DN outburst is usually between 3 and 6, depending upon the orbital period and inclination (Warner 1987; Patterson 2011). An absolute outburst magnitude of 4.5 equates to an orbital period of 4.3 h using the relation in Patterson (2011). We use a Gaussian distribution of absolute magnitudes peaking at 4.5 with a variance of 1.5 mag. To better estimate the effects of different distributions of absolute magnitudes, we reran the simulations with distributions peaking at 5.5 and 3.5 with the same variance. The changes in the detected population of DN outbursts are included in the errors in the final space density and specific frequency estimates.

Because of extinction towards the Bulge, our optical survey would not recover an outburst with $M_V = 4.5$ past a distance of ≈5400 pc. Using a range of peak magnitudes as described above, we expect ≈20 per cent of DNe to be further than this, quickly falling off with almost none as far as 8 kpc. At 5–6 kpc in this longitude, the bulge has started but contributes only ∼15 per cent of the stellar population in this line of sight, though it rises quickly beyond this point. Using models of stellar density from the bulge population compared to the disc population (Pasetto et al. 2012), we find that the effect of including the Bulge in our models will change the number of detected DNe by <10 per cent, much smaller than uncertainties from small number statistics. With a better sample of DNe to work with, it would be worth using a more accurate model of the Milky Way. We have included a 10 per cent additional error in the estimate of specific frequency at the end of the process to address uncertainty from using a simplistic model of the Milky Way.

(iii) The X-ray spectra of CVs are described by a thermal bremsstrahlung model with a characteristic temperature of 15 keV (Mukai et al. 2003). Changing the characteristic temperature of the bremsstrahlung model by, e.g. a factor of 2 up or down makes little difference in the *Chandra* energy band, and thus has little effect on our calculations.

(iv) Extinction is roughly linear with distance (which is certainly not really the case since the lines of sight cross spiral arms, but this is a small source of error compared with the small number statistics), and is calculated assuming the extinction law from Cardelli, Clayton & Mathis (1989), the Vista Variables in Via Lactea reddening maps in Gonzalez et al. (2012), and the relation $N_H = 0.58 \times 10^{22}$ cm^{-2} × $E(B - V)$ found in Bohlin, Savage & Drake (1978), including the observational errors in the extinction maps which can be large in these regions.

(v) X-ray detections of DNe in the GBS are made outside of outburst. This is clearly not accurate – for a 'worst case scenario', we would expect for CVs in the GBS like SS Cyg, which is ∼10 times brighter briefly at the start and end of a DN outburst and a high duty cycle (see Table 1), that about 1/2 would be detected in outburst due to the larger volume sampled, even though the brighter luminosity lasts only ∼10 per cent of the duty cycle (McGowan, Priedhorsky & Trudolyubov 2004). Similarly, more systems like U Gem would be detected in outburst than in quiescence because the higher X-ray flux lasts throughout the duration of the outbursts. A survey that did not premise the detection of the outburst on an X-ray detection would escape this trouble, which could result in somewhat overestimating the specific frequency of CVs.

First, we throw a randomly generated population of CVs on to the region of the sky covered by the GBS and calculate the X-ray flux and optical magnitude of a DN outburst without correcting for extinction. The X-ray luminosities in Byckling et al. (2010) are in a somewhat different energy band than the GBS data. We use WebPimms to correct for this difference using the assumptions about extinction and spectral shape listed above. We similarly correct for the different band used to calculate the X-ray luminosity function from Pretorius & Knigge (2012). If the flux values are above the GBS detection limits, we calculate the duty cycle based on the X-ray luminosity relation above, including the intrinsic scatter around this relation seen in the nine DNe used for the fit. At every point that a relation is invoked, the uncertainty is included as a Gaussian random number with a variance equal to the uncertainty in the relation. We then randomly place an observation at some point in the outburst cycle, and if the observation overlaps with a DN outburst, the DN is provisionally detected. At this point, we look up reddening values for the line of sight each provisionally detected DN is on and calculate extinction in both optical and X-ray, including the observational error in the extinction measures. If the CV remains above the flux limits of the GBS at this point, it is detected. 500 such simulations are run for different values of space density. We find that to generate a population of CVs undergoing DN outbursts consistent with those seen in the GBS, we require a space density of $\rho = 5.6(\pm 3.9) \times 10^{-6}$ pc^{-3} in the solar neighbourhood, scaled up with stellar density as we move closer to the bulge. This is not a measurement of the local space density of high duty cycle CVs; it is a measurement of the density of high duty cycle CVs several kiloparsecs towards the Galactic bulge, and is expressed in terms of the local space density under the assumption that the CV density through the Galaxy traces the stellar population. We write it in this way to allow a more direct comparison to published values of space density. An equivalent, but perhaps easier to
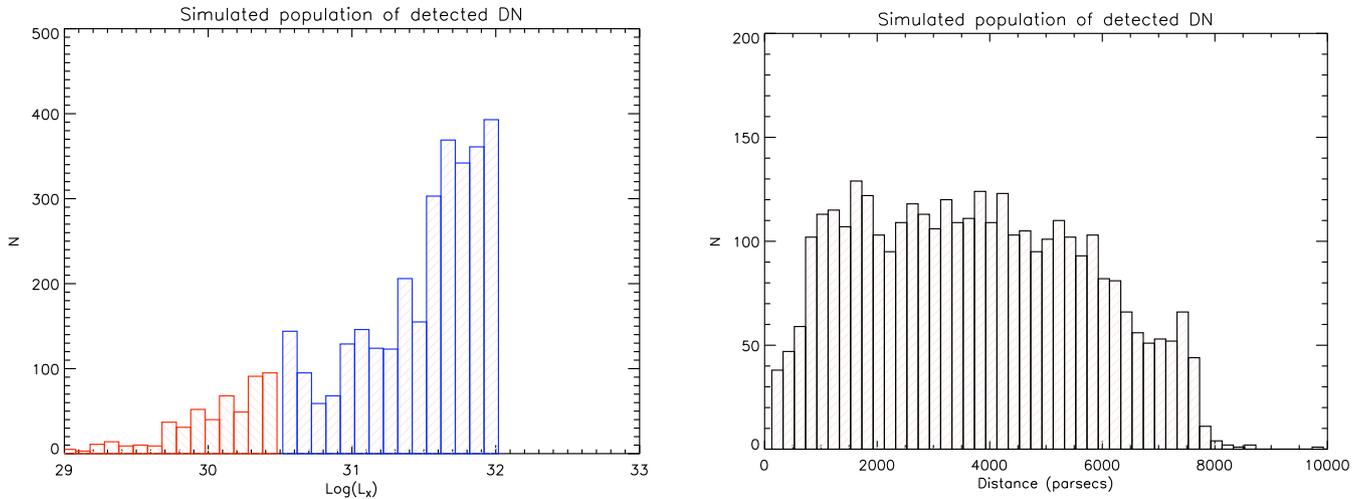
Figure 4. Left: a histogram of the X-ray luminosities of the simulated population of DNe detected by the GBS using the relation between duty cycle and X-ray luminosity derived in Section 2.2. Systems below the break in the Byckling et al. (2010) luminosity function are plotted in red with hatching at $-45°$, while those above are in blue with hatching at $+45°$. 84.8 per cent of systems are above the break. The GBS sample of DNe, therefore, likely is composed primarily of systems of comparable luminosity to those used to fit the relation between duty cycle and X-ray luminosity. Also and importantly, the sample of DNe detected in the GBS is relatively insensitive to the precise shape of the luminosity function, with space density of X-ray luminous CVs playing the major role. This is a result of the short baseline of GBS observations (only 8 d); longer surveys such as Large Synoptic Survey Telescope (LSST) will detect non-magnetic CVs with much lower duty cycles, offering a window into the distribution of the X-ray faint CV population. Right: the simulated distribution of distances of detected DNe. The optical depth of the survey combined with the bright X-ray luminosities expected from the very fact of the outburst detection in such a short baseline results in a distribution that falls off after ∼6 kpc. The primary limit to how far we can detect DN outbursts is the optical brightness of the outburst compared to our survey depth.

visualize, way of writing it is to use the local stellar mass density, $0.085\,M_{\odot}\,pc^{-3}$ (McMillan 2011), to state the average number of CVs per unit stellar mass in the parts of the Galactic disc being probed by the optical GBS survey, $6.6 \pm 4.7 \times 10^{-5}\,M_{\odot}^{-1}$.

This measurement is dominated by the high end of the X-ray luminosity function, as lower luminosity CVs undergo DN outbursts less frequently and are correspondingly less likely to be observed, in addition to the smaller volume reached. In particular, in our simulations of the DN population in the GBS which best match GBS observations only 15.2 per cent of detected DN have X-ray luminosities below the $L_X = 3 \times 10^{30}\,erg\,s^{-1}$ completeness limit of Byckling et al. (2010), as shown in Fig. 4, which would correspond to roughly one of the eight detected DN outbursts in the GBS. As such, the exact shape of the assumed luminosity function at low to moderate luminosities has little effect on the resulting population, and the primary uncertainty comes ultimately from the small number of systems involved at both ends of the simulation. For example, using the luminosity function from Byckling et al. (2010) instead does not have a significant impact on the resulting specific frequency. We also have very little in the way of a lever arm to constrain the relative size of the X-ray faint DN population to the X-ray bright DN population. The space density we measure is a factor of 2 higher than, but is still consistent with, the measurement of local long-period DN in Pretorius & Knigge (2012), $2.1^{+3.5}_{-1.3} \times 10^{-6}\,pc^{-3}$.

5 DISCUSSION

Studies of the space density of CVs have concentrated on the local population, so that the changing density of the stellar environment as one moves outwards radially in the disc is unimportant and generally not considered. In the GBS, however, we likely observe CVs undergoing DN outbursts out to 4–5 kpc. The radial and vertical exponential decay of the stellar density is therefore very important in our estimate of space density in this line of sight. GBS

fields are also particularly close to the plane compared to other measures of space density of CVs which have tried to avoid extinction as much as possible by looking out of the plane of the Milky Way. The concept of a single 'space density' for CVs is one that only makes sense in an extremely local environment where the density is relatively uniform, and is only a useful concept for the population at large in terms of a scale factor to the stellar density.

While the non-uniform structure of the Galaxy is taken into account when calculating the space density of CVs, a more straightforward and ultimately more useful concept may be the specific frequency of CVs, which offers a more direct comparison to population models throughout different regions of the galaxy than the solar environment. The optical photometric follow-up to the GBS (Britt et al. 2014) reached a depth of $r' = 23$. The optical depth of the survey combined with the bright X-ray luminosities expected from the very fact of the outburst detection in such a short baseline results in the distribution shown in the right-hand panel of Fig. 4. This work is therefore a probe of the density of non-magnetic CVs at distances from Earth much greater than any previous survey. Comparing our result to the local space density of long-period CVs reached in Pretorius & Knigge (2012), there is some hint at a higher specific frequency of CVs as one moves in towards the centre of the Galaxy; this is not yet a statistically significant effect, but we have a small number of DNe with which to work and make no attempt to factor in the distances of DNe in the GBS as a result. There is both a theoretical and observational basis to expect a change in specific frequency in different Galactic environments. Kundu, Maccarone & Zepf (2002) show that an increase in the metallicity of Globular Clusters results in an increase in the specific frequency of LMXBs in those clusters. A possible reason for the increase is that donor stars with low metallicities do not develop convective zones at the same stellar mass, and so do not make contact until shorter orbital periods have been reached through other means of angular momentum

loss such as magnetic braking (Ivanova et al. 2006). We consider it likely, therefore, that the specific frequency of CVs should increase towards the Galactic bulge as the metallicity increases, though these data are insufficient to show it.

This work is severely limited by the small number of DNe available for the analysis in both the high-luminosity Byckling sample and in the sample of DNe outbursts detected in the GBS in both optical and X-ray wavelengths. Though the DNe in the GBS sample are all detected in the X-ray, this method is primarily based on DN outburst detection, using the X-ray luminosity function and the connection between X-ray luminosity and duty cycle to connect to a predicted outburst rate. Our agreement with other space density estimates for DNe is a step forward for DN outburst detection methods, as other DN outburst surveys such as Cieslinski et al. (2003) are in disagreement with other methods. Our result does not resolve any apparent tension between empirical and theoretical estimates of CV space density discussed in Section 1, as it agrees well with the majority of other empirical methods.

LSST will offer a much better sampling of DNe systems. LSST will routinely go deeper in all parts of the sky, with frequent sampling and a long baseline that guarantees the detection of thousands of DN outbursts, including those with low duty cycles. Indeed, some large survey work revealing hundreds of new DNe outbursts is already forthcoming (e.g. Drake et al. 2014). Through this work, using large survey data to measure the frequency and brightness of outbursts for thousands of systems can yield an estimate of the relative proportion of CVs over all parts of the sky. Given the consistency of the optical brightness of DN outbursts (Patterson 2011), maps in three dimensions to distances of a few kpc could be made with no observations beyond what LSST is going to take anyway. A similar analysis with Pan-STARRS is complicated by the observing cadence on a similar or longer time-scale than the duration of many DNe outbursts, many of which may only last a matter of days.

The primary uncertainty of our estimate here comes from the small number of systems used, both to establish a quantitative relationship between duty cycle and X-ray luminosity and to match a synthetic population to our eight DNe in the GBS optical campaign of Britt et al. (2014). The former is difficult to improve at present, as the number of X-ray luminous CVs for which highly accurate distances can be measured is small. However, the *GAIA* mission will undoubtedly improve this situation dramatically in several years' time, roughly concurrently with results from LSST (Barstow et al. 2014).

Neither the DN duty cycle nor the X-ray luminosity in quiescence are entirely reliable tracers of the secular mass accretion rate of the system (for which $\dot{M}_1 = -\dot{M}_2$ in conservative mass transfer), as CVs at the same orbital period can exist in states of greatly differing mass transfer rates (e.g. the nova-like below the period gap, BK Lyn; Zellem et al. 2009). Büning & Ritter (2004) suggest that this difference could be due to feedback cycles from irradiation driven mass transfer on the scale of 10^{4-5} yr, but regardless of the mechanism, the disparate instantaneous mass transfer and accretion rates at equal orbital period is an observational fact. Patterson et al. (2013) found that BK Lyn is transitioning to lower mass transfer rates, moving from a nova-like CV to a Z Cam-like state that alternates between a high and a low state, perhaps 'calming down' after an historical nova in AD 101 quickly altered the equilibrium of the system. Z Cam itself could be in a similar transitional period after a nova eruption (Shara et al. 2007). If these periods of high mass transfer only last a few thousand years after a nova, then the majority of systems should have a strong relationship between mass transfer rate and orbital period. Patterson (2011) found that

the recurrence time of DNe below the period gap was strongly a function of mass ratio, with $T_{rec} = 318(\pm30)\,\mathrm{d}\,(q/0.15)^{-2.63\,\pm\,0.17}$. The mass ratio also determines the Roche geometry $\frac{R_L}{a}$ and is strongly related to the WD temperature, itself a function of WD mass and accretion rate (see fig. 10 of Patterson 2011). There is no theoretical prediction of the quiescent instantaneous accretion rate ($\dot{M}_1$) based on system parameters, though these observational signatures are suggestive. Our result may therefore be unsurprising to the community, but is the first quantitative relationship between the duty cycle and X-ray luminosity, and so directly links the average mass transfer rate to the instantaneous accretion rate in quiescence. There is a strong selection effect on orbital period in our sample, as well, since long-period systems have more massive donor stars (Frank, King & Raine 2002) and there is a maximum WD mass. Above the period gap, the mass ratio q must be higher than $q \approx 0.25$, and will have relatively short recurrence times. Long-period systems will therefore be significantly overrepresented in a sample of X-ray luminous, high duty cycle DNe such as those in the GBS, though short-period systems are also sure to be present.

REFERENCES

Aungwerojwit A. et al., 2006, A&A, 455, 659
Barstow M. A. et al., 2014, preprint (arXiv:1407.6163)
Baskill D. S., Wheatley P. J., Osborne J. P., 2001, MNRAS, 328, 71
Bohlin R. C., Savage B. D., Drake J. F., 1978, ApJ, 224, 132
Britt C. T. et al., 2013, ApJ, 769, 120
Britt C. T. et al., 2014, ApJS, 214, 10
Büning A., Ritter H., 2004, A&A, 423, 281
Byckling K., Mukai K., Thorstensen J. R., Osborne J. P., 2010, MNRAS, 408, 2298
Cardelli J. A., Clayton G. C., Mathis J. S., 1989, ApJ, 345, 245
Cieslinski D., Diaz M. P., Mennickent R. E., Pietrzyński G., 2003, PASP, 115, 193
de Kool M., 1992, A&A, 261, 188
Drake A. J. et al., 2014, MNRAS, 441, 1186
Eisenhauer F. et al., 2005, ApJ, 628, 246
Frank J., King A., Raine D. J., 2002, Accretion Power in Astrophysics, 3rd edn. Cambridge Univ. Press, Cambridge
Gonzalez O. A., Rejkuba M., Zoccali M., Valenti E., Minniti D., Schultheis M., Tobar R., Chen B., 2012, A&A, 543, A13
Greiss S., Steeghs D. T. H., Jonker P. G., Torres M. A. P., Maccarone T. J., Hynes R. I., Britt C. T., 2014, MNRAS, 438, 2839
Hamilton R. T., Urban J. A., Sion E. M., Riedel A. R., Voyer E. N., Marcy J. T., Lakatos S. L., 2007, ApJ, 667, 1139
Harrison T. E., Johnson J. J., McArthur B. E., Benedict G. F., Szkody P., Howell S. B., Gelino D. M., 2004, AJ, 127, 460
Henden A. A., 2014, Observations from the AAVSO International Database. Available: http://www.aavso.org
Hynes R. I. et al., 2012, ApJ, 761, 162
Hynes R. I. et al., 2014, ApJ, 780, 11

Ivanova N., Heinke C. O., Rasio F. A., Taam R. E., Belczynski K., Fregeau J., 2006, MNRAS, 372, 1043

Johnson C. B. et al., 2014, MNRAS, 444, 1584

Jonker P. G. et al., 2011, ApJS, 194, 18

Jonker P. G. et al., 2014, ApJS, 210, 18

Jurić M. et al., 2008, ApJ, 673, 864

Kelly B. C., 2007, ApJ, 665, 1489

Kolb U., 1993, A&A, 271, 149

Kundu A., Maccarone T. J., Zepf S. E., 2002, ApJ, 574, L5

Lasota J.-P., 2001, New Astron. Rev., 45, 449

Maccarone T. J. et al., 2012, MNRAS, 426, 3057

McGowan K. E., Priedhorsky W. C., Trudolyubov S. P., 2004, ApJ, 601, 1100

McMillan P. J., 2011, MNRAS, 414, 2446

Markwardt C. B., 2009, in Bohlender D. A., Durand D., Dowler P., eds, ASP Conf. Ser. Vol. 411, Astronomical Data Analysis Software and Systems XVIII. Astron. Soc. Pac., San Francisco, p. 251

Maza J., Gonzalez L. E., 1983, IAU Circ., 3854, 2

Miller-Jones J. C. A., Sivakoff G. R., Knigge C., Körding E. G., Templeton M., Waagen E. O., 2013, Science, 340, 950

Mukai K., Kinkhabwala A., Peterson J. R., Kahn S. M., Paerels F., 2003, ApJ, 586, L77

Oppenheimer B. D., Kenyon S. J., Mattei J. A., 1998, AJ, 115, 1175

Pasetto S. et al., 2012, A&A, 547, A70

Patterson J., 1998, PASP, 110, 1132

Patterson J., 2011, MNRAS, 411, 2695

Patterson J., Raymond J. C., 1985, ApJ, 292, 535

Patterson J. et al., 2013, MNRAS, 434, 1902

Pojmanski G., 1997, Acta Astron., 47, 467

Politano M., 1996, ApJ, 465, 338

Press W. H., Teukolsky S. A., Vetterling W. T., Flannery B. P., 2007, Numerical Recipes, 3rd edn: The Art of Scientific Computing. Cambridge Univ. Press, Cambridge

Pretorius M. L., Knigge C., 2012, MNRAS, 419, 1442

Pretorius M. L., Knigge C., O'Donoghue D., Henry J. P., Gioia I. M., Mullis C. R., 2007, MNRAS, 382, 1279

Ratti E. M. et al., 2013, MNRAS, 428, 3543

Reylé C., Marshall D. J., Robin A. C., Schultheis M., 2009, A&A, 495, 819

Rogel A. B., Cohn H. N., Lugger P. M., 2008, ApJ, 675, 373

Schreiber M. R., Gänsicke B. T., 2003, A&A, 406, 305

Shara M. M. et al., 2007, Nature, 446, 159

Smak J., 1971, Acta Astron., 21, 15

Smak J., 1999, Acta Astron., 49, 391

Swank J. H., Boldt E. A., Holt S. S., Rothschild R. E., Serlemitsos P. J., 1978, ApJ, 226, L133

Thorstensen J. R., 2003, AJ, 126, 3017

Thorstensen J. R., Lépine S., Shara M., 2008, AJ, 136, 2107

Torres M. A. P. et al., 2014, MNRAS, 440, 365

Tremaine S. et al., 2002, ApJ, 574, 740

Warner B., 1987, MNRAS, 227, 23

Warner B., Nather R. E., 1971, MNRAS, 152, 219

Wheatley P. J., Mauche C. W., Mattei J. A., 2000, New Astron. Rev., 44, P33

Williams M. J., Bureau M., Cappellari M., 2010, MNRAS, 409, 1330

Wu J., Jonker P. G., Torres M. A. P., Britt C. T., Hynes R. I., Greiss S., Steeghs D., Maccarone 2015, MNRAS, in press

Zellem R., Hollon N., Ballouz R.-L., Sion E. M., Godon P., Gänsicke B. T., Long K., 2009, PASP, 121, 942

This paper has been typeset from a TEX/LATEX file prepared by the author.